CONDITIONAL POSITIONAL ENCODINGS FOR VISION TRANSFORMERS

Anonymous authors
Paper under double-blind review

ABSTRACT

We propose a conditional positional encoding (CPE) scheme for vision Transformers (Dosovitskiy et al., 2021; Touvron et al., 2020). Unlike previous fixed or learnable positional encodings that are predefined and independent of input tokens, CPE is dynamically generated and conditioned on the local neighborhood of the input tokens. As a result, CPE can easily generalize to the input sequences that are longer than what the model has ever seen during the training. Besides, CPE can keep the desired translation equivalence in vision tasks, resulting in improved performance. We implement CPE with a simple Position Encoding Generator (PEG) to get seamlessly incorporated into the current Transformer framework. Built on PEG, we present Conditional Position encoding Vision Transformer (CPVT). We demonstrate that CPVT has visually similar attention maps compared to those with learned positional encodings and delivers outperforming results.

1 INTRODUCTION

Recently, Transformers (Vaswani et al., 2017) have been viewed as a strong alternative to Convolutional Neural Networks (CNNs) in visual recognition tasks such as classification (Dosovitskiy et al., 2021) and detection (Carion et al., 2020; Zhu et al., 2021). Unlike the convolution operation in CNNs, which has a limited receptive field, the self-attention mechanism in the Transformers can capture the long-distance information and dynamically adapt the receptive field according to the image content. Consequently, Transformers are considered more flexible and powerful than CNNs, being promising to achieve more progress in visual recognition.

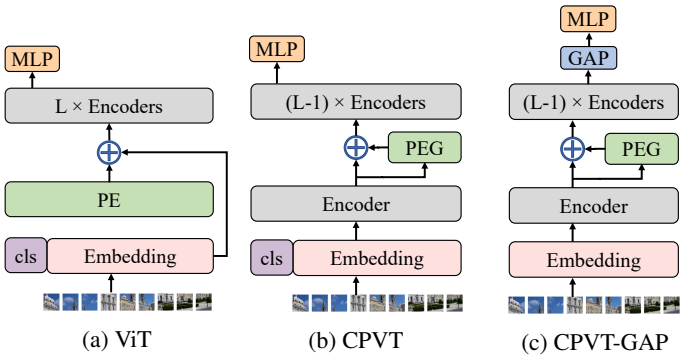

Figure 1. Vision Transformers: (a) ViT (Dosovitskiy et al., 2021) with explicit 1D learnable positional encodings (`PE`) (b) CPVT with conditional positional encoding from the proposed Position Encoding Generator (`PEG`) plugin, which is the *default* choice. (c) CPVT-GAP without class token (`cls`), but with global average pooling (GAP) over all items in the sequence. Note that GAP is a bonus version which has boosted performance.

However, the self-attention operation in Transformers is permutation-invariant, which discards the order of the tokens in an input sequence. To mitigate this issue, previous works (Vaswani et al., 2017; Dosovitskiy et al., 2021) add the absolute positional encodings to each input token (see Figure 1a), which enables order-awareness. The positional encoding can either be learnable or fixed

with sinusoidal functions of different frequencies. Despite being effective, these positional encodings seriously harm the flexibility of the Transformers, hampering their broader applications. Taking the learnable version as an example, the encodings are often a vector of equal length to the input sequence, which are jointly updated with the network weights during training. As a result, the length and the value of the positional encodings are fixed once trained. During testing, it causes difficulties of handling the sequences longer than the ones in the training data.

The inability to adapt to longer input sequences during testing greatly limits the range of generalization. For instance, in vision tasks like object detection, we expect the model can be applied to the images of any size during inference, which might be much larger than the training images. A possible remedy is to use bicubic interpolation to upsample the positional encodings to the target length, but it degrades the performance without fine-tuning as later shown in our experiments. For vision in general, we expect that the models be translation-equivariant. For example, the output feature maps of CNNs shift accordingly as the target objects are moved in the input images. However, the absolute positional encoding scheme breaks the translation equivalence because it adds unique positional encodings to each token (or each image patch). One may overcome the issue with relative positional encodings as in (Shaw et al., 2018). However, relative positional encodings not only come with extra computational costs, but also require modifying the implementation of the standard Transformers. Last but not least, the relative positional encodings cannot work equally well as the absolute ones, because the image recognition task still requires absolute position information (Islam et al., 2020), which the relative positional encodings fail to provide.

In this work, we advocate a novel positional encoding (PE) scheme to incorporate the position information into Transformers. Unlike the predefined and input-agnostic positional encodings used in previous works (Dosovitskiy et al., 2021; Vaswani et al., 2017; Shaw et al., 2018), the proposed PE is dynamically generated and conditioned on the local neighborhood of input tokens. Thus, our positional encodings can change along with the input size and can keep translation equivalence. We demonstrate that the vision transformers (Dosovitskiy et al., 2021; Touvron et al., 2020) with our new PE (*i.e*. CPVT, see Figure 1c) achieve even better performance. We summarize our contributions as,

- We propose a novel positional encoding (PE) scheme, termed *conditional position encodings* (CPE). CPE is dynamically generated with Positional Encoding Generators (PEG) and can be effortlessly implemented by the modern deep learning frameworks (Paszke et al., 2019; Abadi et al., 2016; Chen et al., 2015), requiring no changes to the current Transformer APIs.
- As opposed to widely-used absolute positional encodings, CPE can keep the *translation equivalence* which is important to improve the performance of Transformers. Moreover, for image classification tasks we employ the global average pooling (GAP, also translation-invariant) to replace the default class token (Dosovitskiy et al., 2021). Our use of GAP in ViT is prior to Swin (Liu et al., 2021) and it further improves the performance by **1%**.
- Built on CPE, we propose Conditional Position encoding Vision Transformer (CPVT). It achieves better performance than previous vison transformers (Dosovitskiy et al., 2021; Touvron et al., 2020).
- CPE is adaptable to arbitrary input sizes, which are required in many important downstream tasks such as segmentation and detection. Through experiments we show that CPE can boost the segmentation and detection performance for a recent pyramid transformer (Wang et al., 2021) by a clear margin.

2 Related Work

2.1 Vision Transformers

Transformer (Vaswani et al., 2017) has achieved great success in natural language processing (NLP) and it is used in many state-of-the-art models such as BERT (Devlin et al., 2019), GPT (Radford et al., 2018; 2019), and GPT-3 (Brown et al., 2020). Due to the flexibility of the transformer, recent works attempt to apply it to vision tasks such as classification (Dosovitskiy et al., 2021; Touvron et al., 2020). It has been shown that the self-attention module is able to replace the convolution operation (Ramachandran et al., 2019), since self-attention layers can attend pixel-grid patterns similarly to the CNN layers (Cordonnier et al., 2020). One of the issues is that applying self-attention to

vision tasks may lead to huge computational costs because an image may have tens of thousands of pixels. ViT (Dosovitskiy et al., 2021) bypasses the issue by splitting an image into patches. Specifically, it decomposes a 224×224 image into a series of 196 flattened patches (16×16 pixels each), which are analogous to a sequence of words in language processing. Based on ViT, DeiT (Touvron et al., 2020) further makes the transformers more data-efficient, and it can be directly trained on ImageNet. Besides, Transformer is used to solve other vision tasks such as detection (Carion et al., 2020; Zhu et al., 2021), segmentation (Wang et al., 2020; Zheng et al., 2020), image generation (Parmar et al., 2018), and low-level tasks (Chen et al., 2020). We give preliminary knowledge in A.

2.2 Positional Encodings

Since self-attention itself is permutation-equivariant (see A.3), positional encodings are commonly employed to incorporate the order of sequences (Vaswani et al., 2017). The positional encodings can either be fixed or learnable, while either being absolute or relative. Vision transformers follow the same fashion to imbue the network with positional information.

Absolute Positional Encoding. The absolute positional encoding is the most widely used. In the original transformer (Vaswani et al., 2017), the encodings are generated with the sinusoidal functions of different frequencies and then they are added to the inputs. Alternatively, the positional encodings can be learnable, where they are implemented with a fixed-dimension matrix/tensor and jointly updated with the model's parameters with SGD.

Relative Positional Encoding. The relative position encoding (Shaw et al., 2018) considers distances between the tokens in the input sequence. Compared to the absolute ones, the relative positional encodings can be translation-equivariant and can naturally handle the sequences longer than the longest sequences during training (*i.e.*, being inductive). A 2-D relative position encoding is proposed for image classification in (Bello et al., 2019), showing superiority to 2D sinusoidal embeddings. The relative positional encoding is further improved in XLNet (Yang et al., 2019b) and DeBERTa (He et al., 2020), showing better performance.

Other forms. Complex-value embeddings (Wang et al., 2019) are an extension to model global absolute encodings and show improvement. RoFormer (Su et al., 2021) utilizes a rotary position embedding to encode both absolute and relative position information for text classification. FLOATER (Liu et al., 2020) proposes a novel continuous dynamical model to capture position encodings. It is not limited by the maximum sequence length during training, meanwhile being parameter-efficient.

Similar designs to CPE. Convolutions are used to model local relations in ASR and machine translation (Gulati et al., 2020; Mohamed et al., 2019; Yang et al., 2019a; Yu et al., 2018). However, they are mainly limited to 1D signals. We instead process 2D vision images.

3 Vision Transformer with Conditional Position Encodings

3.1 Motivation

In vision transformers, an input image of size $H \times W$ is split into patches with size $S \times S$, the number of patches is $N = \frac{HW}{S^2}$ [1]. The patches are added with the same number of learnable absolute positional encoding vectors. In this work, we argue that the positional encodings used here have two issues. First, it prevents the model from handling the sequences longer than the learnable PE. Second, it makes the model not translation-equivariant because a unique positional encoding vector is added to every one patch. The translation equivalence plays an important role in classification because we hope the networks' responses changes accordingly as the object moves in the image.

One may note that the first issue can be remedied by removing the positional encodings since except for the positional encodings, all other components (*e.g.*, MHSA and FFN) of the vision transformer can directly be applied to longer sequences. However, this solution severely deteriorates the performance. This is understandable because the order of the input sequence is an important clue and the

[1] H and W shall be divisible by S, respectively.

model has no way to extract the order without the positional encodings. The experiment results on ImageNet are shown in Table 1. By removing the positional encodings, DeiT-tiny's performance on ImageNet dramatically degrades from 72.2% to 68.2%.

Table 1. Comparison of various positional encoding (PE) strategies tested on ImageNet validation set in terms of the top-1 accuracy. Removing the positional encodings greatly damages the performance. The relative postional encodings have inferior performance to the absolute ones

Model	Encoding	Top-1@224(%)	Top-1@384(%)
DeiT-tiny (Touvron et al., 2020)	✗	68.2	68.6
DeiT-tiny (Touvron et al., 2020)	learnable	72.2	71.2
DeiT-tiny (Touvron et al., 2020)	sin-cos	72.3	70.8
DeiT-tiny	2D RPE (Shaw et al., 2018)	70.5	69.8

Second, in DeiT (Touvron et al., 2020), they show that we can interpolate the position encodings to make them have the same length of the longer sequences. However, this method requires fine-tuning the model a few more epochs, otherwise the performance will remarkably drop, as shown in Table 1. This goes contrary to what we would expect. With the higher-resolution inputs, we often expect a remarkable performance improvement without any fine-tuning. Finally, the relative position encodings (Shaw et al., 2018; Bello et al., 2019) can cope with both the aforementioned issues. However, the relative positional encoding cannot provide *absolute position information*, which is also important to the classification performance (Islam et al., 2020). As shown in Table 1, the model with relative position encodings has inferior performance (70.5% vs. 72.2%).

3.2 Conditional Positional Encodings

We argue that a successful positional encoding for vision tasks should meet these requirements,

(1) Making the input sequence *permutation-variant* but *translation-equivariant*.

(2) Being inductive and able to handle the sequences longer than the ones during training.

(3) Having the ability to provide the absolute position to a certain degree. This is important to the performance as shown in (Islam et al., 2020).

In this work, we find that characterizing the local relationship by positional encodings is sufficient to meet all of the above. First, it is *permutation-variant* because the permutation of input sequences also affects the order in some local neighborhoods. However, translation of an object in an input image does not change the order in its local neighborhood, *i.e.*, *translation-equivariant* (see Section A.3). Second, the model can easily generalize to longer sequences since only the local neighborhoods of a token are involved. Besides, if the absolute position of any input token is known, the absolute position of all the other tokens can be inferred by the mutual relation between input tokens. We will show that the tokens on the borders can be aware of their absolute positions due to the commonly-used zero paddings.

Therefore, we propose *positional encoding generators* (PEG) to dynamically produce the positional encodings conditioned on the local neighborhood of an input token.

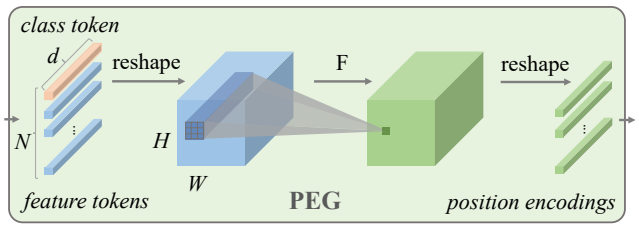

Figure 2. Schematic illustration of Positional Encoding Generator (PEG). Note d is the embedding size, N is the number of tokens.

Positional Encoding Generator. PEG is illustrated in Figure 2. To condition on the local neighbors, we first reshape the flattened input sequence $X \in \mathbb{R}^{B \times N \times C}$ of DeiT back to $X' \in \mathbb{R}^{B \times H \times W \times C}$ in the 2-D image space. Then, a function (denoted by $\mathcal{F}$ in Figure 2) is repeatedly applied to the local patch in X' to produce the conditional positional encodings $E^{B \times H \times W \times C}$. PEG can be efficiently implemented with a 2-D convolution with kernel k ($k \geq 3$) and $\frac{k-1}{2}$ zero paddings. Note that the

zero paddings here are important to make the model be aware of the absolute positions, and $\mathcal{F}$ can be of various forms such as a various types of convolutions and many others.

3.3 Conditional Positional Encoding Vision Transformers

Built on the conditional positional encodings, we propose our Conditional Positional Encoding Vision Transformers (CPVT). Except that our positional encodings are conditional, we exactly follow ViT and DeiT to design our vision transformers and we also have three sizes CPVT-Ti, CPVT-S and CPVT-B. Similar to the original positional encodings in DeiT, the conditional positional encodings are also added to the input sequence, as shown in Figure 1 (b). In CPVT, the position where PEG is applied is also important to the performance, which will be studied in the experiments.

In addition, both DeiT and ViT utilize an extra learnable class token to perform classification (*i.e.*, `cls_token` shown in Figure 1 (a) and (b)). By design, the class token is not translation-invariant although it can learn to be so. A simple alternative is to directly replace it with a global average pooling (GAP), which is inherently translation-invariant, resulting in our CVPT-GAP. Together with the translation-equivariant positional encodings, CVPT-GAP is uttermost translation-invariant and thus can achieve much better image classification performance.

4 Experiments

4.1 Setup

Datasets. Following DeiT (Touvron et al., 2020), we use ILSVRC-2012 ImageNet dataset (Deng et al., 2009) with 1K classes and 1.3M images to train all our models. We report the results on the validation set with 50K images. Unlike ViT (Dosovitskiy et al., 2021), we do not use the much larger undisclosed JFT-300M dataset (Sun et al., 2017).

Model variants. We have three models with various sizes to adapt to various computing scenarios. The detailed settings are shown in Table 8 (see B.1). All experiments in this paper are performed on Tesla V100 machines. Training the tiny model for 300 epochs takes about 1.3 days on a single node with 8 V100 GPU cards. CPVT-S and CPVT-B take about 1.6 and 2.5 days, respectively.

Training details All the models (except for CPVT-B) are trained for 300 epochs with a global batch size of 2048 on Tesla V100 machines using AdamW optimizer (Loshchilov & Hutter, 2019). We don't tune the hyper-parameters and strictly comply with the settings in DeiT (Touvron et al., 2020). The learning rate is scaled with this formula $lr_{scale} = \frac{0.0005 * BatchSize_{global}}{512}$. The detailed hyperparameters are in the B.2.

4.2 Generalization to Higher Resolutions

As mentioned before, our proposed PEG can directly generalize to larger image sizes without any fine-tuning. We confirm this here by evaluating the models trained with 224×224 images on the $384 \times 384, 448 \times 448, 512 \times 512$ images. The results are shown in Table 2. With the 384×384 input images, The DeiT-tiny with learnable positional encodings degrades from 72.2% to 71.2%. When equipped with sine encoding, the tiny model degrades from 72.2% to 70.8%. In constrat, CPVT model with the proposed PEG can directly process the larger input images, and CPVT-Ti's performance is boosted from 73.4% to 74.2% when applied to 384×384 images. Our CPVT-Ti outperforms DeiT-tiny by 3.0%. This gap continues to increase as the input resolution enlarges.

4.3 CPVT with Global Average Pooling

By design, the proposed PEG is translation-equivariant. Thus, if we further use the translation-invariant global average pooling (GAP) instead of the `cls_token` before the final classification layer of CPVT. CPVT can be totally translation-invariant, which should be beneficial to the ImageNet classification task. Note the using GAP here results in even less computation complexity because we do not need to compute the attention interaction between the class token and the image patches. As shown in Table 3, using GAP here can boost CPVT by more than **1%**. For example, equipping CPVT-Ti with GAP obtains 74.9% top-1 accuracy on ImageNet validation dataset, which

Table 2. Direct evaluation on other resolutions without fine-tuning. The models are trained on 224×224. A simple PEG of a single layer of 3×3 depth-wise convolution is used here

Model	Params	160(%)	224(%)	384(%)	448(%)	512(%)
DeiT-tiny	6M	65.6	72.2	71.2	68.8	65.9
DeiT-tiny (sin)	6M	65.2	72.3	70.8	68.2	65.1
DeiT-tiny (no pos)	6M	62.1	68.2	68.6	68.4	65.0
CPVT-Ti	6M	66.8(+1.2)	72.4(+0.2)	73.2(+2.0)	71.8(+3.0)	70.3(+4.4)
CPVT-Ti ‡	6M	67.7 (+2.1)	73.4(+1.2)	74.2(+3.0)	72.6(+3.8)	70.8(+4.9)
DeiT-small	22M	75.6	79.9	78.1	75.9	72.6
CPVT-S	22M	76.1(+0.5)	79.9	80.4(+1.5)	78.6(+2.7)	76.8(+4.2)
DeiT-base	86M	79.1	81.8	79.7	79.8	78.2
CPVT-B	86M	80.5(+1.4)	81.9(+0.1)	82.3(+2.6)	82.4(+2.6)	81.0(+2.8)

‡: Insert one PEG each after the first encoder till the fifth encoder

outperforms DeiT-tiny by a large margin (+2.7%). Moreover, it even exceeds DeiT-tiny model with distillation (74.5%). In contrast, DeiT with GAP cannot gain so much improvement (only 0.4% as shown in Table 3) because the original absolute PE is not translation-equivariant and GAP with the PE is not translation-invariant. Given the superior performance, we hope our model can be a strong alternative in vision transformers.

Table 3. Performance comparison of Class Token (CLT) and global average pooling (GAP) on ImageNet. CPVT's can be further boosted with GAP

Model	Head	Params	Top-1 Acc (%)	Top-5 Acc (%)
DeiT-tiny (Touvron et al., 2020)	CLT	6M	72.2	91.0
DeiT-tiny	GAP	6M	72.6	91.2
CPVT-Ti ‡	CLT	6M	73.4	91.8
CPVT-Ti ‡	GAP	6M	**74.9**	**92.6**
DeiT-small (Touvron et al., 2020)	CLT	22M	79.9	95.0
DeiT-small	GAP	22M	80.2	95.2
CPVT-S ‡	CLT	23M	80.5	95.2
CPVT-S ‡	GAP	23M	**81.5**	**95.7**

‡: Insert one PEG each after the first encoder till the fifth encoder

4.4 Complexity of PEG

Few Parameters. Given the model dimension d, the extra number of parameters introduced by PEG is $d \times l \times k^2$ if we choose l depth-wise convolutions with kernel k. Even if we use l separable convolutions, this value becomes $l(d^2 + k^2 d)$. When $k = 3$ and $l = 1$, CPVT-Ti ($d = 192$) brings about 1, 728 parameters. Note that DeiT-tiny utilizes learnable position encodings with $192 \times 14 \times 14 = 37632$ parameters. Therefore, CPVT-Ti has 35, 904 fewer number of parameters than DeiT-tiny. Even using 4 layers of separable convolutions, CPVT-Ti introduces only $38952 - 37632 = 960$ more parameters, which is negelectable compared to the 5.7M model parameters of DeiT-tiny.

FLOPs. As for FLOPs, l layers of $k \times k$ depth-wise convolutions possesses $14 \times 14 \times d \times l \times k^2$ FLOPS. Taking the tiny model for example, it involves $196 \times 192 \times 9 = 0.34M$ FLOPS for the simple case $k = 3, l = 1$, which is neglectable because the model has 2.1G FLOPs in total.

4.5 Qualitative Analysis of CPVT

Thus far, we have shown that PEG can have better performance than the original positional encodings. However, because PEG provides the position in an implicit way, it is interesting to see if PEG can indeed provide the position information as the original positional encodings. Here we investigate this by visualizing the attention weights of the transformers. Specifically, given a 224×224 image (i.e. 14×14 patches), the score matrix within a single head is 196×196. We visualize the normalized self-attention score matrix of the second encoder block.

We first visualize the attention weights of DeiT with the original positional encodings. As shown in Figure 3 (middle), the diagonal element interacts strongly with its local neighbors but weakly with those far-away elements, which suggests that DeiT with the original positional encodings learn to attend the local neighbors of each patch. After the positional encodings are removed (denoted by DeiT w/o PE), all the patches produce similar attention weights and fail to attend to the patches near themselves, see Figure 3 (left).

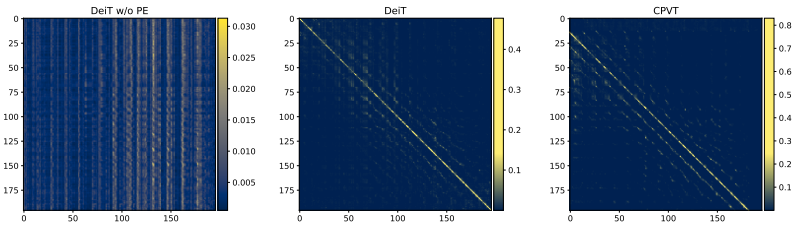

Figure 3. Normalized attention scores (first head) of the second encoder block of DeiT without position encoding (DeiT w/o PE), DeiT (Touvron et al., 2020), and CPVT on the same input sequence. Position encodings are key to developing a schema of locality in lower layers of DeiT. Meantime, CPVT profits from conditional encodings and follows a similar locality pattern.

Finally, we show the attention weights of our CPVT model with PEG. As shown in Figure 3 (right), like the original positional encodings, the model with PEG can also learn a similar attention pattern, which indicates that the proposed PEG can provide the position information as well.

4.6 Comparison with State-of-the-art Methods

We evaluate the performance of CPVT models on the ImageNet validation dataset and report the results in Table 4. Compared with DeiT, *CPVT models have much better top-1 accuracy with similar throughputs*. Our models can enjoy performance improvement when inputs are upscaled without fine-tuning, while DeiT degrades as discussed in Table 2, see also Figure 4 for a clear comparison. Noticeably, Our model with GAP marks a new state-of-the-art for vision Transformers.

We further train CPVT-Ti and DeiT-tiny using the aforementioned training settings plus the hard distillation proposed in (Touvron et al., 2020). Specifically, we use RegNetY-160 (Radosavovic et al., 2020) as the teacher. CPVT obtains 75.9%, exceeding DeiT-tiny by 1.4%.

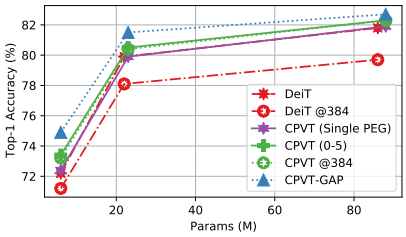

Figure 4. Comparison of CPVT and DeiT models under various configurations. Notice that DeiT@384 performs worse than at default 224 input size. In contrast, CPVT@384 has improved performance. More PEGs can result in better performance. CPVT-GAP performs the best.

4.7 PEG on Pyramid Transformer Architectures

PVT (Wang et al., 2021) is a recently-proposed vision transformer with the multi-stage design like ResNet (He et al., 2016). Swin (Liu et al., 2021) is a follow-up work and comes with higher performance. We apply our method on both to demonstrate its generalization ability.

ImageNet classification. Specifically, we remove its learnable PE and apply our PEG in position 0 of each stage with a GAP head. We use the same training settings to make a fair comparison and show the results in Table 12. Our method can significantly boost PVT-tiny by 3.1% and Swin-tiny by 1.15% on ImageNet (c.f. B.5). We also evaluate the performance of PEG on some downstream semantic segmentation and object detection tasks (see B.6). Note these tasks usually handle the various input resolutions as the training because multi-scale data augmentation is extensively used.

Table 4. Comparison with ConvNets and Transformers on ImageNet and ImageNet Real (Beyer et al., 2020). CPVT have much better performance compared with prior Transformers

Models	Params(M)	Input	throughput*	ImNet top-1 %	Real top-1 %
ResNet-50 (He et al., 2016)	25	224^2	1226.1	76.2	82.5
ResNet-101 (He et al., 2016)	45	224^2	753.6	77.4	83.7
ResNet-152 (He et al., 2016)	60	224^2	526.4	78.3	84.1
RegNetY-4GF (Radosavovic et al., 2020)	21	224^2	1156.7	80.0	86.4
EfficientNet-B0 (Tan & Le, 2019)	5	224^2	2694.3	77.1	83.5
EfficientNet-B1 (Tan & Le, 2019)	8	240^2	1662.5	79.1	84.9
EfficientNet-B2 (Tan & Le, 2019)	9	260^2	1255.7	80.1	85.9
EfficientNet-B3 (Tan & Le, 2019)	12	300^2	732.1	81.6	86.8
EfficientNet-B4 (Tan & Le, 2019)	19	380^2	349.4	82.9	88.0
ViT-B/16 (Dosovitskiy et al., 2021)	86	384^2	85.9	77.9	-
ViT-L/16	307	384^2	27.3	76.5	-
DeiT-tiny w/o PE (Touvron et al., 2020)	6	224^2	2536.5	68.2	-
DeiT-tiny (Touvron et al., 2020)	6	224^2	2536.5	72.2	80.1
DeiT-tiny (sine)	6	224^2	2536.5	72.3	80.3
CPVT-Ti ‡	6	224^2	2500.7	73.4	81.3
CPVT-Ti-GAP‡	6	224^2	2520.1	**74.9**	82.5
DeiT-tiny (Touvron et al., 2020)⚗	6	224^2	2536.5	74.5	82.1
CPVT-Ti⚗	6	224^2	2500.7	**75.9**	83.0
DeiT-small (Touvron et al., 2020)	22	224^2	940.4	79.9	85.7
CPVT-S ‡	23	224^2	930.5	80.5	86.0
CPVT-S-GAP‡	23	224^2	942.3	**81.5**	86.6
DeiT-base (Touvron et al., 2020)	86	224^2	292.3	81.8	86.7
CPVT-B ‡	88	224^2	285.5	82.3	87.0
CPVT-B-GAP‡	88	224^2	290.2	**82.7**	87.7

*: Measured in *img/s* on a 16GB V100 GPU as in (Touvron et al., 2020).
‡: Insert one PEG each after the first encoder till the fifth encoder
⚗: trained with hard distillation using RegNetY-160 as the teacher.

5 Ablation Study

5.1 Positional encoding or merely a hybrid?

One might suspect that the PEG's improvement comes from the extra *learnable parameters* introduced by the convolutional layers in PEG, instead of the local relationship retained by PEG. One way to test the function of PEG is only adding it when calculating Q and K in the attention layer, so that only the positional information of PEG is passed through. We can achieve 71.3% top-1 accuracy on ImageNet with DeiT-tiny. This is significantly better than DeiT-tiny w/o PE (68.2%) and is similar to the one with PEG on Q, K and V (72.4%), which suggests that PEG mainly serves as a positional encoding scheme.

We also design another experiment to remove this concern. By randomly-initializing a 3×3 PEG and fixing its weights during the training, we can obtain 71.3% accuracy (Table 5), which is much higher (3.1%↑) than DeiT without any PE (68.2%). Since the weights of PEG are fixed and the performance improvement can only be due to the introduced position information. On the contrary, when we exhaustively use 12 convolutional layers (kernel size being 1, *i.e.*, not producing local relationship) to replace the PEG, these layers have much more learnable parameters than PEG. However, it only boosts the performance by 0.4% to 68.6%.

Table 5. Positional encoding rather than added parameters gives the most improvement

Kernel	Style	Params (M)	Top-1 Acc (%)
none	-	5.68	68.2
3	fixed (random init)	5.68	71.3
3	fixed (learned init)	5.68	72.3
1 (12 ×)	learnable	6.13	68.6
3	learnable	5.68	**72.4**

Another interesting finding is that fixing a learned PEG also helps training. When we initialize with a learned PEG instead of the random values and train the tiny version of the model from scratch

while keeping the PEG fixed, the model can also achieve 72.3% top-1 accuracy on ImageNet. This is very close to the learnable PEG (72.4%).

5.2 PEG POSITION IN CPVT

We also experiment by varying the position of the PEG in the model. Table 6 left presents the ablations for variable positions based on the tiny model. *We denote the input of the first encoder by index -1*. Therefore, position 0 is the output of the first encoder block. PEG shows strong performance ($\sim$72.4%) when it is placed at [0, 3].

Note that positioning the PEG at 0 can have much better performance than positioning it at -1 (*i.e.*, before the first encoder), as shown in Table 6 left. We observe that the difference between the two situations is they have different receptive fields. Specifically, the former has a global field while the latter can only see a local area. Hence, *they are supposed to work similarly well if we enlarge the convolution's kernel size*. To verify our hypothesis, we use a quite large kernel size 27 with a padding size 13 at position -1, whose result is reported in Table 6 right. It achieves similar performance to the one positioning the PEG at 0 (72.5%), which verifies our assumption.

Table 6. Comparison of different plugin positions (left) and different kernels (right) using DeiT-tiny

Position Idx	Top-1 Acc(%)	Top-5 Acc(%)
none	68.2	88.7
-1	70.6	90.2
0	**72.4**	**91.2**
3	72.3	91.1
6	71.7	90.8
10	69.0	89.1

PosIdx	kernel	Params	Top-1 Acc(%)	Top-5 Acc(%)
-1	3×3	5.7M	70.6	90.2
-1	27×27	5.8M	**72.5**	**91.3**

5.3 COMPARISONS WITH OTHER POSITIONAL ENCODINGS

We compare PEG with other commonly used encodings: absolute positional encoding (e.g. sinusoidal (Vaswani et al., 2017)), *relative positional encoding* (RPE) (Shaw et al., 2018) and *learnable encoding* (LE) (Devlin et al., 2019; Radford et al., 2018), as shown in Table 7.

DeiT-tiny obtains 72.2% with learnable absolute PE. We experiment with the 2-D sinusoidal encodings to achieve on-par performance. For RPE, we follow (Shaw et al., 2018) and set the local range hyper-parameter K as 8, with which we obtain 70.5%. RPE here does not encode any absolute position information, see discussion in D.1 and B.3.

Moreover, we combine the learnable absolute PE with a single-layer PEG. This boosts the baseline CPVT-Ti (0-1) by 0.5. If we use 4-layer PEG, it can achieve 72.9%. Moreover, if we add a single layer PEG to the first five blocks, we can obtain 73.4%, which indicates that it is better to add the positional encodings to different blocks than stacking them at one.

Table 7. Comparison of various positional encoding strategies. LE: learnable positional encoding. RPE: relative positional encoding

Model	PEG Pos	Encoding	Top-1 (%)	Top-5 (%)
DeiT-tiny (2020)	-	LE	72.2	91.0
DeiT-tiny	-	2D sin-cos	72.3	91.0
DeiT-tiny	-	2D RPE	70.5	90.0
CPVT-Ti	0-1	PEG	72.4	91.2
CPVT-Ti	0-1	PEG + LE	72.9	91.4
CPVT-Ti	0-1	$4\times$PEG + LE	72.9	91.4
CPVT-Ti	0-5	PEG	**73.4**	**91.8**

6 CONCLUSION

We introduced CPVT, a novel method to provide the position information in vision Transformers, which dynamically generates the position encodings based on the local neighbors of each input token. Through extensive experimental studies, we demonstrate that our proposed positional encodings can achieve stronger performance than the previous positional encodings. The transformer models with our positional encodings can naturally process longer input sequences and keep the desired translation equivalence in vision tasks. Moreover, our positional encodings are easy to implement and come with negligible cost. We look forward to a broader application of our method in transformer-driven vision tasks like segmentation and video processing.

REFERENCES

Martín Abadi, Paul Barham, Jianmin Chen, Zhifeng Chen, Andy Davis, Jeffrey Dean, Matthieu Devin, Sanjay Ghemawat, Geoffrey Irving, Michael Isard, et al. Tensorflow: A system for large-scale machine learning. In *12th {USENIX} symposium on operating systems design and implementation ({OSDI} 16)*, pp. 265–283, 2016.

Irwan Bello. Lambdanetworks: Modeling long-range interactions without attention. In *International Conference on Learning Representations*, 2021. URL `https://openreview.net/forum?id=xTJEN-ggl1b`.

Irwan Bello, Barret Zoph, Ashish Vaswani, Jonathon Shlens, and Quoc V Le. Attention augmented convolutional networks. In *Proceedings of the IEEE/CVF International Conference on Computer Vision*, pp. 3286–3295, 2019.

Lucas Beyer, Olivier J Hénaff, Alexander Kolesnikov, Xiaohua Zhai, and Aäron van den Oord. Are we done with imagenet? *arXiv preprint arXiv:2006.07159*, 2020.

Tom B Brown, Benjamin Mann, Nick Ryder, Melanie Subbiah, Jared Kaplan, Prafulla Dhariwal, Arvind Neelakantan, Pranav Shyam, Girish Sastry, Amanda Askell, et al. Language models are few-shot learners. *arXiv preprint arXiv:2005.14165*, 2020.

Nicolas Carion, Francisco Massa, Gabriel Synnaeve, Nicolas Usunier, Alexander Kirillov, and Sergey Zagoruyko. End-to-end object detection with transformers. In *European Conference on Computer Vision*, pp. 213–229. Springer, 2020.

Hanting Chen, Yunhe Wang, Tianyu Guo, Chang Xu, Yiping Deng, Zhenhua Liu, Siwei Ma, Chunjing Xu, Chao Xu, and Wen Gao. Pre-trained image processing transformer. *arXiv preprint arXiv:2012.00364*, 2020.

Tianqi Chen, Mu Li, Yutian Li, Min Lin, Naiyan Wang, Minjie Wang, Tianjun Xiao, Bing Xu, Chiyuan Zhang, and Zheng Zhang. Mxnet: A flexible and efficient machine learning library for heterogeneous distributed systems. *arXiv preprint arXiv:1512.01274*, 2015.

Jean-Baptiste Cordonnier, Andreas Loukas, and Martin Jaggi. On the relationship between self-attention and convolutional layers. In *International Conference on Learning Representations*, 2020.

Ekin Dogus Cubuk, Barret Zoph, Jon Shlens, and Quoc Le. Randaugment: Practical automated data augmentation with a reduced search space. *Advances in Neural Information Processing Systems*, 33, 2020.

Zihang Dai, Hanxiao Liu, Quoc Le, and Mingxing Tan. Coatnet: Marrying convolution and attention for all data sizes. *Advances in Neural Information Processing Systems*, 34, 2021.

Jia Deng, Wei Dong, Richard Socher, Li-Jia Li, Kai Li, and Li Fei-Fei. Imagenet: A large-scale hierarchical image database. In *2009 IEEE conference on computer vision and pattern recognition*, pp. 248–255. Ieee, 2009.

Jacob Devlin, Ming-Wei Chang, Kenton Lee, and Kristina Toutanova. Bert: Pre-training of deep bidirectional transformers for language understanding. In *Proceedings of the 2019 Conference of the North American Chapter of the Association for Computational Linguistics: Human Language Technologies, Volume 1 (Long and Short Papers)*, pp. 4171–4186, 2019.

Alexey Dosovitskiy, Lucas Beyer, Alexander Kolesnikov, Dirk Weissenborn, Xiaohua Zhai, Thomas Unterthiner, Mostafa Dehghani, Matthias Minderer, Georg Heigold, Sylvain Gelly, Jakob Uszkoreit, and Neil Houlsby. An image is worth 16x16 words: Transformers for image recognition at scale. In *International Conference on Learning Representations*, 2021. URL `https://openreview.net/forum?id=YicbFdNTTy`.

Stéphane d'Ascoli, Hugo Touvron, Matthew L Leavitt, Ari S Morcos, Giulio Biroli, and Levent Sagun. Convit: Improving vision transformers with soft convolutional inductive biases. In *International Conference on Machine Learning*, pp. 2286–2296. PMLR, 2021.

Anmol Gulati, James Qin, Chung-Cheng Chiu, Niki Parmar, Yu Zhang, Jiahui Yu, Wei Han, Shibo Wang, Zhengdong Zhang, Yonghui Wu, et al. Conformer: Convolution-augmented transformer for speech recognition. *arXiv preprint arXiv:2005.08100*, 2020.

Kaiming He, Xiangyu Zhang, Shaoqing Ren, and Jian Sun. Deep residual learning for image recognition. In *Proceedings of the IEEE conference on computer vision and pattern recognition*, pp. 770–778, 2016.

Pengcheng He, Xiaodong Liu, Jianfeng Gao, and Weizhu Chen. Deberta: Decoding-enhanced bert with disentangled attention. *arXiv preprint arXiv:2006.03654*, 2020.

Elad Hoffer, Tal Ben-Nun, Itay Hubara, Niv Giladi, Torsten Hoefler, and Daniel Soudry. Augment your batch: Improving generalization through instance repetition. In *Proceedings of the IEEE/CVF Conference on Computer Vision and Pattern Recognition*, pp. 8129–8138, 2020.

Cheng-Zhi Anna Huang, Ashish Vaswani, Jakob Uszkoreit, Noam Shazeer, Ian Simon, Curtis Hawthorne, Andrew M Dai, Matthew D Hoffman, Monica Dinculescu, and Douglas Eck. Music transformer. In *Advances in Neural Processing Systems*, 2018.

Gao Huang, Yu Sun, Zhuang Liu, Daniel Sedra, and Kilian Q Weinberger. Deep networks with stochastic depth. In *European conference on computer vision*, pp. 646–661. Springer, 2016.

Md Amirul Islam, Sen Jia, and Neil DB Bruce. How much position information do convolutional neural networks encode? In *International Conference on Learning Representations*, 2020.

Alexander Kirillov, Ross Girshick, Kaiming He, and Piotr Dollár. Panoptic feature pyramid networks. In *Proceedings of the IEEE/CVF Conference on Computer Vision and Pattern Recognition*, pp. 6399–6408, 2019.

Tsung-Yi Lin, Priya Goyal, Ross Girshick, Kaiming He, and Piotr Dollár. Focal loss for dense object detection. In *Proceedings of the IEEE international conference on computer vision*, pp. 2980–2988, 2017.

Xuanqing Liu, Hsiang-Fu Yu, Inderjit Dhillon, and Cho-Jui Hsieh. Learning to encode position for transformer with continuous dynamical model. In *International Conference on Machine Learning*, pp. 6327–6335. PMLR, 2020.

Ze Liu, Yutong Lin, Yue Cao, Han Hu, Yixuan Wei, Zheng Zhang, Stephen Lin, and Baining Guo. Swin transformer: Hierarchical vision transformer using shifted windows. *arXiv preprint arXiv:2103.14030*, 2021.

Ilya Loshchilov and Frank Hutter. Decoupled weight decay regularization. In *International Conference on Learning Representations*, 2019. URL `https://openreview.net/forum?id=Bkg6RiCqY7`.

Abdelrahman Mohamed, Dmytro Okhonko, and Luke Zettlemoyer. Transformers with convolutional context for asr. *arXiv preprint arXiv:1904.11660*, 2019.

Niki Parmar, Ashish Vaswani, Jakob Uszkoreit, Lukasz Kaiser, Noam Shazeer, Alexander Ku, and Dustin Tran. Image transformer. In Jennifer Dy and Andreas Krause (eds.), *Proceedings of the 35th International Conference on Machine Learning*, volume 80 of *Proceedings of Machine Learning Research*, pp. 4055–4064, Stockholmsmässan, Stockholm Sweden, 10–15 Jul 2018. PMLR.

Adam Paszke, Sam Gross, Francisco Massa, Adam Lerer, James Bradbury, Gregory Chanan, Trevor Killeen, Zeming Lin, Natalia Gimelshein, Luca Antiga, et al. Pytorch: An imperative style, high-performance deep learning library. *Advances in Neural Information Processing Systems*, 32: 8026–8037, 2019.

Alec Radford, Karthik Narasimhan, Tim Salimans, and Ilya Sutskever. Improving language understanding by generative pre-training. 2018.

Alec Radford, Jeffrey Wu, Rewon Child, David Luan, Dario Amodei, and Ilya Sutskever. Language models are unsupervised multitask learners. *OpenAI blog*, 1(8):9, 2019.

Ilija Radosavovic, Raj Prateek Kosaraju, Ross Girshick, Kaiming He, and Piotr Dollár. Designing network design spaces. In *Proceedings of the IEEE/CVF Conference on Computer Vision and Pattern Recognition*, pp. 10428–10436, 2020.

Prajit Ramachandran, Niki Parmar, Ashish Vaswani, Irwan Bello, Anselm Levskaya, and Jon Shlens. Stand-alone self-attention in vision models. In H. Wallach, H. Larochelle, A. Beygelzimer, F. d'Alché-Buc, E. Fox, and R. Garnett (eds.), *Advances in Neural Information Processing Systems*, volume 32, pp. 68–80. Curran Associates, Inc., 2019. URL https://proceedings.neurips.cc/paper/2019/file/3416a75f4cea9109507cacd8e2f2aefc-Paper.pdf.

Peter Shaw, Jakob Uszkoreit, and Ashish Vaswani. Self-attention with relative position representations. In *Proceedings of the 2018 Conference of the North American Chapter of the Association for Computational Linguistics: Human Language Technologies, Volume 2*, pp. 464–468, 2018.

Nitish Srivastava, Geoffrey Hinton, Alex Krizhevsky, Ilya Sutskever, and Ruslan Salakhutdinov. Dropout: a simple way to prevent neural networks from overfitting. *The journal of machine learning research*, 15(1):1929–1958, 2014.

Jianlin Su, Yu Lu, Shengfeng Pan, Bo Wen, and Yunfeng Liu. Roformer: Enhanced transformer with rotary position embedding. *arXiv preprint arXiv:2104.09864*, 2021.

Chen Sun, Abhinav Shrivastava, Saurabh Singh, and Abhinav Gupta. Revisiting unreasonable effectiveness of data in deep learning era. In *Proceedings of the IEEE international conference on computer vision*, pp. 843–852, 2017.

Christian Szegedy, Vincent Vanhoucke, Sergey Ioffe, Jon Shlens, and Zbigniew Wojna. Rethinking the inception architecture for computer vision. In *Proceedings of the IEEE conference on computer vision and pattern recognition*, pp. 2818–2826, 2016.

Mingxing Tan and Quoc Le. Efficientnet: Rethinking model scaling for convolutional neural networks. In *International Conference on Machine Learning*, pp. 6105–6114. PMLR, 2019.

Hugo Touvron, Matthieu Cord, Matthijs Douze, Francisco Massa, Alexandre Sablayrolles, and Hervé Jégou. Training data-efficient image transformers & distillation through attention. *arXiv preprint arXiv:2012.12877*, 2020.

Ashish Vaswani, Noam Shazeer, Niki Parmar, Jakob Uszkoreit, Llion Jones, Aidan N Gomez, Łukasz Kaiser, and Illia Polosukhin. Attention is all you need. In *Proceedings of the 31st International Conference on Neural Information Processing Systems*, pp. 6000–6010, 2017.

Benyou Wang, Donghao Zhao, Christina Lioma, Qiuchi Li, Peng Zhang, and Jakob Grue Simonsen. Encoding word order in complex embeddings. *arXiv preprint arXiv:1912.12333*, 2019.

Wenhai Wang, Enze Xie, Xiang Li, Deng-Ping Fan, Kaitao Song, Ding Liang, Tong Lu, Ping Luo, and Ling Shao. Pyramid vision transformer: A versatile backbone for dense prediction without convolutions. *arXiv preprint arXiv:2102.12122*, 2021.

Yuqing Wang, Zhaoliang Xu, Xinlong Wang, Chunhua Shen, Baoshan Cheng, Hao Shen, and Huaxia Xia. End-to-end video instance segmentation with transformers. *arXiv preprint arXiv:2011.14503*, 2020.

Haiping Wu, Bin Xiao, Noel Codella, Mengchen Liu, Xiyang Dai, Lu Yuan, and Lei Zhang. Cvt: Introducing convolutions to vision transformers. *arXiv preprint arXiv:2103.15808*, 2021.

Baosong Yang, Longyue Wang, Derek Wong, Lidia S Chao, and Zhaopeng Tu. Convolutional self-attention networks. *arXiv preprint arXiv:1904.03107*, 2019a.

Zhilin Yang, Zihang Dai, Yiming Yang, Jaime Carbonell, Ruslan Salakhutdinov, and Quoc V Le. Xlnet: Generalized autoregressive pretraining for language understanding. *arXiv preprint arXiv:1906.08237*, 2019b.

Adams Wei Yu, David Dohan, Minh-Thang Luong, Rui Zhao, Kai Chen, Mohammad Norouzi, and Quoc V Le. Qanet: Combining local convolution with global self-attention for reading comprehension. *arXiv preprint arXiv:1804.09541*, 2018.

Sangdoo Yun, Dongyoon Han, Seong Joon Oh, Sanghyuk Chun, Junsuk Choe, and Youngjoon Yoo. Cutmix: Regularization strategy to train strong classifiers with localizable features. In *Proceedings of the IEEE/CVF International Conference on Computer Vision*, pp. 6023–6032, 2019.

Hongyi Zhang, Moustapha Cisse, Yann N. Dauphin, and David Lopez-Paz. mixup: Beyond empirical risk minimization. In *International Conference on Learning Representations*, 2018. URL `https://openreview.net/forum?id=r1Ddp1-Rb`.

Sixiao Zheng, Jiachen Lu, Hengshuang Zhao, Xiatian Zhu, Zekun Luo, Yabiao Wang, Yanwei Fu, Jianfeng Feng, Tao Xiang, Philip HS Torr, et al. Rethinking semantic segmentation from a sequence-to-sequence perspective with transformers. *arXiv preprint arXiv:2012.15840*, 2020.

Zhun Zhong, Liang Zheng, Guoliang Kang, Shaozi Li, and Yi Yang. Random erasing data augmentation. In *Proceedings of the AAAI Conference on Artificial Intelligence*, volume 34, pp. 13001–13008, 2020.

Bolei Zhou, Hang Zhao, Xavier Puig, Sanja Fidler, Adela Barriuso, and Antonio Torralba. Scene parsing through ade20k dataset. In *Proceedings of the IEEE conference on computer vision and pattern recognition*, pp. 633–641, 2017.

Xizhou Zhu, Weijie Su, Lewei Lu, Bin Li, Xiaogang Wang, and Jifeng Dai. Deformable detr: Deformable transformers for end-to-end object detection. In *International Conference on Learning Representations*, 2021. URL `https://openreview.net/forum?id=gZ9hCDWe6ke`.

A PRELIMINARY KNOWLEDGE

Transformer (Vaswani et al., 2017) features a series of encoders and decoders of an identical structure. Every encoder and decoder has a *multi-head self-attention layer* (MHSA) and a *feed-forward network layer* (FFN), while each decoder has an extra attention layer to process the output of the encoder. Positional encodings instills position information for a sequence of input tokens.

A.1 TRANSFORMER COMPONENTS

Self-attention. An attention function on input $x = \{x_1, \ldots, x_n\}$ is computed simultaneously on a set of queries Q with keys K and values V by the following,

$$\begin{aligned} \mathrm{Att}(x) &= \mathrm{softmax}(\frac{Q \cdot K^\top}{\sqrt{d_k}}) \cdot V \\ Q = W^Q x, K &= W^K x, V = W^V x \end{aligned} \tag{1}$$

where W^Q, W^K, and W^V are weight matrices to generate Q, K, and V via linear transformations on x. And $Q \cdot K^\top$ calculates attention score as the dot product of the query and all the keys, scaled by the dimension d_k of keys K.

Multi-head Self-Attention. First, Q, K, and V are linearly projected for h times with different learned weights. Then the self-attention function is applied in parallel to generate h outputs, so-called *heads*. All heads are concatenated to give the final output, *i.e.*,

$$\begin{aligned} \mathrm{MultiHead}(Q, K, V) &= \mathrm{Concat}(\mathrm{head_1}, ..., \mathrm{head_h})W^O \\ \text{where} \quad \mathrm{head_i} &= \mathrm{Att}(QW_i^Q, KW_i^K, VW_i^V) \end{aligned} \tag{2}$$

Feed-forward network. The attention output is typically processed by a two-layer linear transformation with an activation in between,

$$FFN(x) = max(0, W_1 x + b_1)W_2 + b_2 \tag{3}$$

Layer Normalization. A residual function and a layer normalization is added for each of the sub-layers (*e.g.*, attention layer and feed-forward layer) in every encoder and decoder, *i.e.*, $\mathrm{LayerNorm}(x + \mathrm{Sublayer}(x))$.

A.2 POSITIONAL ENCODINGS

Positional Encoding. Transformer (Vaswani et al., 2017) adopts a sinusoidal function to encode positions, e.g.

$$\begin{aligned} PE(pos, 2i) &= \sin(pos/10000^{2i/d_{\text{model}}}) \\ PE(pos, 2i+1) &= \cos(pos/10000^{2i/d_{\text{model}}}) \end{aligned} \tag{4}$$

where pos denotes the word position in the sequence, d_{model} means the total encoding dimension, and i is the current dimension. However, the position can also be encoded as relative positional encodings (RPE) (Shaw et al., 2018). Formally,

$$\begin{aligned} \mathrm{Att}(x_i) &= \sum_{j=1}^{n} \alpha_{ij}(W^V x_j + a_{ij}^V) \\ \alpha_{ij} &= \frac{\exp e_{ij}}{\sum_{k=1}^{n} \exp e_{ik}}, e_{ij} = \frac{x_i W^Q (x_j W^K + a_{ij}^K)^T}{\sqrt{d_k}} \end{aligned} \tag{5}$$

where $a_{ij} \in \mathbb{R}^{d_k}$ denotes edge distances between x_i and x_j when seeing input elements as a directed and fully-connected graph. RPE creates practical space complexity for implementation, which require more efficient version as in (Huang et al., 2018). Moreover, it also requires substantial intrusion into standard Transformer APIs.

A.3 TRANSLATION EQUIVARIANCE

The term translation-equivariance means the output feature maps can be equally translated with the input signal. Imagine there is a person in the left-top of an image, if the person is moved to the right-bottom, the output feature maps will change accordingly. This property is very important to the success of convolution network. Convolution (ignoring paddings), RPE, and self-attention are all translation-equivariant operations (regardless of their receptive field). It's nontrivial to make absolute positional encodings like DeiT (using learnable positional encoding) translation-equivariant since different absolute positions will be added if the input signal is translated.

B EXPERIMENT DETAILS

B.1 ARCHITECTURE VARIANTS OF CPVT

Table 8. CPVT architecture variants. The larger model, CPVT-B, has the same architecture as ViT-B (Dosovitskiy et al., 2021) and DeiT-B (Touvron et al., 2020). CPVT-S and CPVT-Ti have the same architecture as DeiT-small and DeiT-tiny respectively

Model	#channels	#heads	#layers	#params
CPVT-Ti	192	3	12	6M
CPVT-S	384	6	12	22M
CPVT-B	768	12	12	86M

B.2 THE HYPERPARAMETERS OF CPVT

As for the ImageNet classification task, we use exactly the same hyperparameters as DeiT, as detailed in Table 9.

Table 9. Hyper-parameters for ViT-B, DeiT-B and CPVT

Methods	ViT-B	DeiT-B	CPVT
Epochs	300	300	300
Batch size	4096	1024	1024
Optimizer	AdamW	AdamW	AdamW
Learning rate decay	cosine	cosine	cosine
Weight decay	0.3	0.05	0.05
Warmup epochs	3.4	5	5
Label smoothing ε (Szegedy et al., 2016)	✗	0.1	0.1
Dropout (Srivastava et al., 2014)	0.1	✗	✗
Stoch. Depth (Huang et al., 2016)	✗	0.1	0.1
Repeated Aug (Hoffer et al., 2020)	✗	✓	✓
Gradient Clip.	✓	✗	✗
Rand Augment (Cubuk et al., 2020)	✗	9/0.5	9/0.5
Mixup prob. (Zhang et al., 2018)	✗	0.8	0.8
Cutmix prob. (Yun et al., 2019)	✗	1.0	1.0
Erasing prob. (Zhong et al., 2020)	✗	0.25	0.25

B.3 IMPORTANCE OF ZERO PADDINGS

We design an experiment to verify the importance of the *zero paddings*, which can help the model infer the absolute positional information. Specifically, we use CPVT-S and simply remove the zero paddings from CPVT while keeping all other settings unchanged. Table 10 shows that this can only obtain 70.5%, which indicates that the zero paddings and absolute positional information play important roles in classifying objects.

Table 10. Ablation study on ImageNet performance w/ or w/o zero paddings

Model	Padding	Top-1 Acc(%)	Top-5 Acc(%)
CPVT-Ti	✓	**72.4**	**91.2**
	✗	70.5	89.8

B.4 SINGLE PEG VS. MULTIPLE PEGS

We further evaluate whether or not using *multi-position* encodings can benefit the performance in Table 11. Notice we denote by i-j the inserted positions of PEG which start from the i-th encoder and end at the $j-1$-th one (inclusion). By inserting PEGs to five positions, the top-1 accuracy of the tiny model can achieve 73.4%, which surpasses DeiT-tiny by 1.2%. Similarly, CPVT-S can achieve 80.5%. It turns out more PEGs do help, but up to a level where more PEGs become incremental (0-5 vs. 0-11).

Table 11. CPVT's sensitivity to number of plugin positions

Positions	Model	Params (M)	Top-1 Acc (%)	Top-5 Acc (%)
0-1	tiny	5.7	72.4	91.2
0-5	tiny	5.9	**73.4**	**91.8**
0-11	tiny	6.1	**73.4**	**91.8**
0-1	small	22.0	79.9	95.0
0-5	small	22.9	80.5	**95.2**
0-11	small	23.8	**80.6**	**95.2**

B.5 CLASSFICATION EVALUATION OF SWIN WITH PEG

We show the validation curves when training Swin (Liu et al., 2021) equipped with PEG in Figure 5. It can boost Swin-tiny from 81.10% to 82.25% (+1.15%↑) on ImageNet.

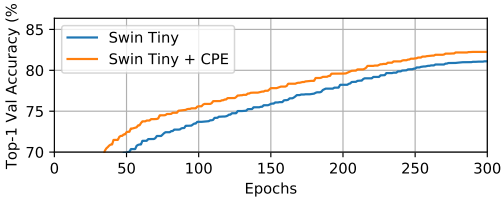

Figure 5. CPE boosts Swin Tiny on ImageNet by 1.15% top-1 Acc.

B.6 EVALUATION ON SEGMENTATION AND DETECTION

Semantic segmentation on ADE20K. We evaluate the performance of PEG on the ADE20K (Zhou et al., 2017) segmentation task. Based on the Semantic FPN framework (Kirillov et al., 2019), PVT achieves much better results than ResNet (He et al., 2016) baselines. Under carefully controlled settings, PEG further boosts PVT-tiny by 3.1% mIoU.

Object detection on COCO. We also perform controlled experiments with the RetinaNet (Lin et al., 2017) framework on the COCO detection task. The results are shown in Table 12. In the standard $1\times$ schedule, PEG improves PVT-tiny by 2.0% mAP. PEG brings 2.4% higher mAP under the $3\times$ schedule.

Table 12. Our method boosts the performance of PVT on ImageNet classification, ADE20K segmentation and COCO detection

Backbone	ImageNet		Semantic FPN on ADE20K		RetinaNet on COCO		
	Params (M)	Top-1 (%)	Params (M)	mIoU (%)	Params (M)	mAP (%, 1×)	mAP (%, 3×, +MS)
ResNet-18 (He et al., 2016)	12	69.8	16	32.9	21	31.8	35.4
PVT-tiny (Wang et al., 2021)	13	75.0	17	35.7	23	36.7	39.4
PVT-tiny+PEG	13	77.3	17	38.0	23	38.0	**41.8**
PVT-tiny+GAP	13	75.9	17	36.0	23	36.9	39.7
PVT-tiny+PEG+GAP	13	**78.1**	17	**38.8**	23	**38.7**	**41.8**
PVT-small (Wang et al., 2021)	25	79.8	28	39.8	34	40.4	42.2
PVT-small+PEG+GAP	25	**81.2**	28	**44.3**	34	**43.0**	**45.2**
PVT-Medium (Wang et al., 2021)	44	81.2	48	41.6	54	41.9	43.2
PVT-Medium+PEG+GAP	44	**82.7**	48	**44.9**	54	**44.3**	**46.4**

B.7 Ablation on Other Forms of PEG

We explore several forms of PEG based on the tiny model, which change the type of convolution, kernel size and layers. The inserted position is 0. The result is shown in Table 13. When we use large kernel of 7×7 or dense convolution, the performance improvement is limited. Stacking more layers of depth-wise convolution doesn't bring significant improvement. Therefore, we use the simplest form as our default implementation. It indicates that this design is enough to provide good position information.

Table 13. Other forms of PEG. The simple form of a single depth-wise 3×3 is good enough.

Variants	Model	Top-1 Acc (%)
1 Depthwise Conv 3×3	tiny	72.4
1 Depthwise Conv 7×7	tiny	72.5
4 * (Depthwise Conv 3×3 +BN+ReLU)	tiny	72.4
1 Dense Conv 3×3	tiny	72.3
4 * (Dense Conv 3×3+BN+ReLU)	tiny	72.5

C Example Code

C.1 PEG

In the simplest form, we use a single depth-wise convolution and show its usage in Transformer by the following PyTorch snippet. Through experiments, we find that such a simple design (*i.e.*, depth-wise 3×3) readily achieves on par or even better performance than the recent SOTAs. We give the torch implementation example in Alg. 1.

D More discussions

D.1 Why RPE works less well than absolute PE?

As mentioned in Section 5.3 (main text), RPE is inferior to the absolute positional encoding. It is because RPE does not encode any absolute position information. Also discussed in Section B.3 (main text), absolute position information is also important even for ImageNet classification, as it is needed to determine which object is at the center of the image. Note that there might be multiple objects in an image, and the label of an image is the category of the object at the center.

Additionally, although RPE becomes popular recently, it is often jointly used with absolute positional encodings (e.g., in ConViT (d'Ascoli et al., 2021)), or the absolute position information is leaked in other ways (e.g., convolution paddings in CoAtNet (Dai et al., 2021)). This further suggests absolute position information is crucial.

Algorithm 1 PyTorch snippet of PEG.

```
import torch
import torch.nn as nn
class VisionTransformer:
 def __init__(layers=12, dim=192, nhead=3, img_size=224, patch_size=16):
   self.pos_block = PEG(dim)
   self.blocks = nn.ModuleList([TransformerEncoderLayer(dim, nhead, dim*4) for _ in range(
       layers)])
   self.patch_embed = PatchEmbed(img_size, patch_size, dim*4)
 def forward_features(self, x):
   B, C, H, W = x.shape
   x, patch_size = self.patch_embed(x)
   _H, _W = H // patch_size, W // patch_size
   x = torch.cat((self.cls_tokens, x), dim=1)
   for i, blk in enumerate(self.blocks):
     x = blk(x)
     if i == 0:
       x = self.pos_block(x, _H, _W)
   return x[:, 0]


class PEG(nn.Module):
 def __init__(self, dim=2\textsc{56}, k=3):
   self.pos = nn.Conv2d(dim, dim, k, 1, k//2, groups=dim) # Only for demo use, more
       complicated functions are effective too.
 def forward(self, x, H, W):
   B, N, C = x.shape
   cls_token, feat_tokens = x[:, 0], x[:, 1:]
   feat_tokens = feat_tokens.transpose(1, 2).view(B, C, H, W)
   x = self.pos(feat_tokens) + feat_tokens
   x = x.flatten(2).transpose(1, 2)
   x = torch.cat((cls_token.unsqueeze(1), x), dim=1)
   return x
```

D.2 Comparison to Lambda Networks

Our work is also related to Lambda Networks (Bello, 2021) which uses 2D relative positional encodings. We evaluate its lambda module with an embedding size of 128, where we denote its encoding scheme as RPE2D-d128. Noticeably, this configuration has about 5.9M parameters (comparable to DeiT-tiny) but only obtains 68.7%. We attribute its failure to the limited ability in capturing the correct positional information. After all, lambda layers are designed with the help of many CNN backbones components such as down-sampling to form various stages, to replace ordinary convolutions in ResNet (He et al., 2016). In contrast, CPVT is transformer-based.

E Extra Figures

E.1 Attention Scores

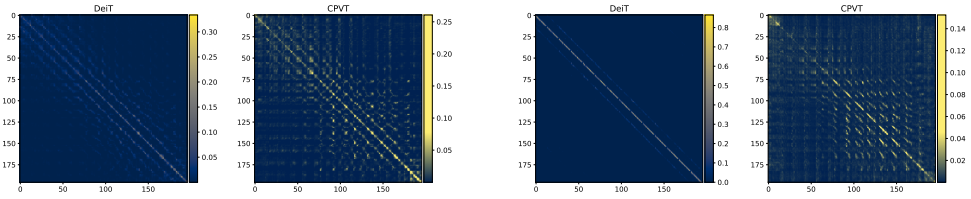

(a) The second head (b) The third head

Figure 6. Normalized attention scores (the second and third head) of the second encoder block of DeiT (Touvron et al., 2020), and CPVT on the same input sequence. DeiT and CPVT share similar locality patterns that are aligned diagonally.

E.2 Comparison with Other Approaches

We further compare our method with other approaches such as CvT Wu et al. (2021), ConViT d'Ascoli et al. (2021) and CoAtNetDai et al. (2021) on ImageNet validation set in Table 14. To

make fair comparisons, we categorize these methods into two groups: plain and pyramid models. Since our models are primarily for plain models, we adapt our methods on two popular pyramid frameworks PVT and Swin. Our CPVT-S-GAP slightly outperforms ConViT-S by 0.2% with 4M fewer parameters and 0.8G fewer FLOPs. When equipped with pyramid designs, our methods are still comparable to CvT and CoAtNet.

Table 14. Performance comparison with other approaches such as CvT Wu et al. (2021), ConViT d'Ascoli et al. (2021) and CoAtNetDai et al. (2021) on ImageNet validation set. All the models are trained on ImageNet-1k dataset and tested on the validation set using 224$\times$224 resolution.

Model	Type	Params	FLOPs	Top-1 Acc (%)
DeiT-small (Touvron et al., 2020)	Plain	22M	4.6G	79.9
ConViT-S (d'Ascoli et al., 2021)	Plain	27M	5.4G	81.3
CPVT-S-GAP (ours)	Plain	23M	4.6G	**81.5**
CoAtNet-0 (Dai et al., 2021)	Pyramid	25M	4.2G	81.6
CvT-13 (Wu et al., 2021)	Pyramid	20M	4.5G	81.6
PVT-small (Wang et al., 2021)	Pyramid	25M	3.8G	79.8
PVT-small+PEG+GAP	Pyramid	25M	3.8G	81.2
Swin-tiny (Liu et al., 2021)	Pyramid	29M	4.5G	81.3
Swin-tiny+PEG+GAP	Pyramid	29M	4.5G	**82.3**